Predicting post-resection recurrence by integrating imaging-based surrogates of distinct vascular patterns of hepatocellular carcinoma

Authors

Xiang-Pan Meng, Tian-Yu Tang, Yongping Zhou, Cong Xia, Tianyi Xia, Yibing Shi, Xueying Long, Yun Liang, Wenbo Xiao, Yuan-Cheng Wang, Xiangming Fang, Shenghong Ju

Correspondence

jsh@seu.edu.cn (S. Ju).

Graphical abstract

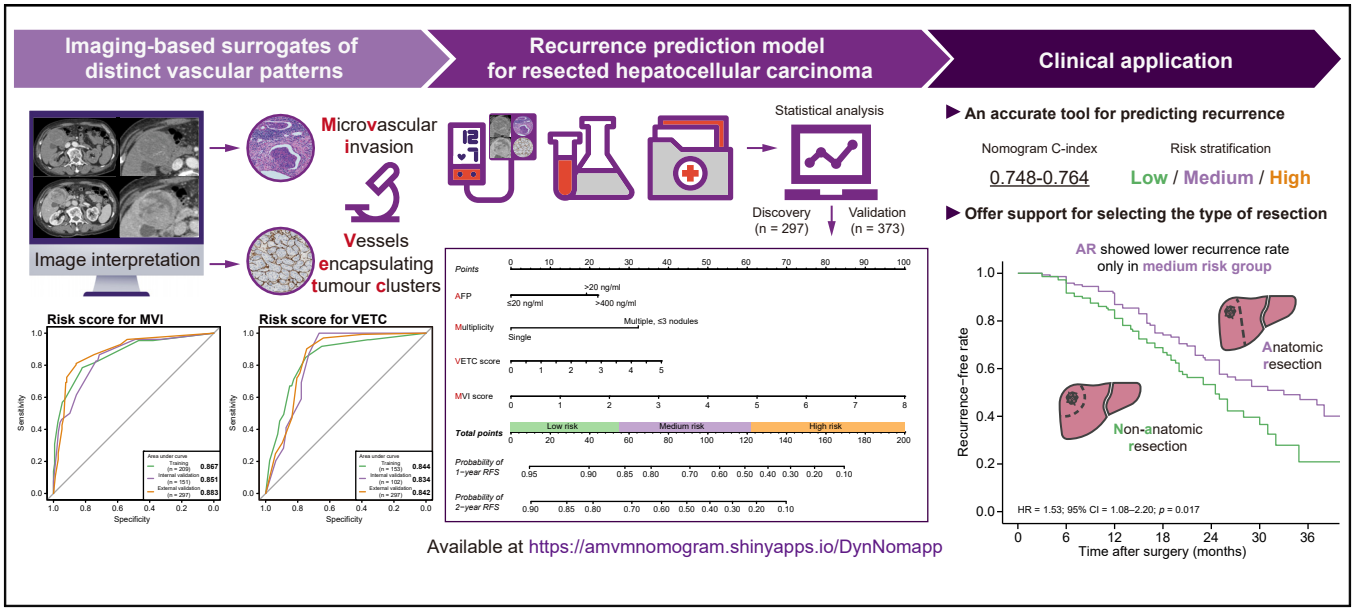

Highlights

- CT features were effective at estimating microvascular invasion and vessels encapsulating tumour clusters (VETC) patterns.
- Nomogram incorporating both imaging surrogates showed informative recurrence prediction.
- The nomogram may facilitate allocation of surgical candidates with hepatocellular carcinoma to the optimal type of resection.

Impact and implications

MVI and VETC are distinct vascular patterns of HCC associated with aggressive biological behaviour and poor outcomes. Our multicentre study provided a model incorporating imaging-based surrogates of these patterns for preoperatively predicting RFS. The proposed model, which uses imaging detection to estimate the risk of MVI and VETC, offers an opportunity to help shed light on the association between tumour aggressiveness and prognosis and to support the selection of the appropriate type of surgical resection.

https://doi.org/10.1016/j.jhepr.2023.100806

Research article

JHEP|Reports

Predicting post-resection recurrence by integrating imaging-based surrogates of distinct vascular patterns of hepatocellular carcinoma

Xiang-Pan Meng,[1] Tian-Yu Tang,[1] Yongping Zhou,[2] Cong Xia,[1] Tianyi Xia,[1] Yibing Shi,[3] Xueying Long,[4] Yun Liang,[5] Wenbo Xiao,[6] Yuan-Cheng Wang,[1] Xiangming Fang,[7] Shenghong Ju[1,*]

[1]*Department of Radiology, Jiangsu Key Laboratory of Molecular and Functional Imaging, Zhongda Hospital, Medical School of Southeast University, Nanjing, China;* [2]*Department of Hepatobiliary Surgery, Jiangnan University Medical Center, Wuxi, China;* [3]*Department of Radiology, The Affiliated Xuzhou Center Hospital of Southeast University, Xuzhou, China;* [4]*Department of Radiology, The Xiangya Hospital of Central South University, Changsha, China;* [5]*Department of Hepatic-Biliary-Pancreatic Center, The First Affiliated Hospital of Kunming Medical University, Kunming, China;* [6]*Department of Radiology, The First Affiliated Hospital, College of Medicine, Zhejiang University, Hangzhou, China;* [7]*Department of Radiology, The Affiliated Wuxi People's Hospital of Nanjing Medical University, Wuxi, China*

JHEP Reports **2023.** https://doi.org/10.1016/j.jhepr.2023.100806

Background & Aims: Distinct vascular patterns, including microvascular invasion (MVI) and vessels encapsulating tumour clusters (VETC), are associated with poor outcomes of hepatocellular carcinoma (HCC). Imaging surrogates of these vascular patterns potentially help to predict post-resection recurrence. Herein, a prognostic model integrating imaging-based surrogates of these distinct vascular patterns was developed to predict postoperative recurrence-free survival (RFS) in patients with HCC.

Methods: Clinico-radiological data of 1,285 patients with HCC from China undergoing surgical resection were retrospectively enrolled from seven medical centres between 2014 and 2020. A prognostic model using clinical data and imaging-based surrogates of MVI and VETC patterns was developed (n = 297) and externally validated (n = 373) to predict RFS. The surrogates (i.e. MVI and VETC scores) were individually built from preoperative computed tomography using two independent cohorts (n = 360 and 255). Whether the model's stratification was associated with postoperative recurrence following anatomic resection was also evaluated.

Results: The MVI and VETC scores demonstrated effective performance in their respective training and validation cohorts (AUC: 0.851–0.883 for MVI and 0.834–0.844 for VETC). The prognostic model incorporating serum alpha-foetoprotein, tumour multiplicity, MVI score, and VETC score achieved a C-index of 0.748–0.764 for the developing and external validation cohorts and generated three prognostically distinct strata. For patients at model-predicted medium risk, anatomic resection was associated with improved RFS (p <0.05). By contrast, anatomic resection had no impact on RFS in patients at model-predicted low or high risk (both p >0.05).

Conclusions: The proposed model integrating imaging-based surrogates of distinct vascular patterns enabled accurate prediction for RFS. It can potentially be used to identify HCC surgical candidates who may benefit from anatomic resection.

Impact and implications: MVI and VETC are distinct vascular patterns of HCC associated with aggressive biological behaviour and poor outcomes. Our multicentre study provided a model incorporating imaging-based surrogates of these patterns for preoperatively predicting RFS. The proposed model, which uses imaging detection to estimate the risk of MVI and VETC, offers an opportunity to help shed light on the association between tumour aggressiveness and prognosis and to support the selection of the appropriate type of surgical resection.

Introduction

Liver cancer is currently the third leading cause of cancer deaths globally, and hepatocellular carcinoma (HCC) represents 75–85% of primary liver cancer.[1,2] Among the various therapeutic options, surgical resection is the mainstay of curative treatment options in China, comprising nearly half of all new patients globally.[2,3] However, the outcomes of hepatic resection remain unsatisfactory owing to frequent recurrence.[4] Considering the current rates of recurrence, preoperative risk stratification for guiding therapeutic options is still suboptimal. There is, thus, a need for identification of novel prognosticators to improve prognostic stratification.

Since most HCC recurrence is attributed to occult metastasis from the primary tumour, tumour characteristics, including

Keywords: Hepatocellular carcinoma; Liver resection; Microvascular invasion; Modelling; Recurrence.

Received 4 April 2023; received in revised form 8 May 2023; accepted 10 May 2023; available online 1 June 2023

* Corresponding author. Address: Department of Radiology, Jiangsu Key Laboratory of Molecular and Functional Imaging, Zhongda Hospital, Medical School of Southeast University, 87 Dingjiaqiao Road, Nanjing 210009, China; Tel.: +86 25 8327 2121.

E-mail address: jsh@seu.edu.cn (S. Ju).

morphologic and pathologic factors, are considered the most unneglectable informative prognostic indicators after resection.[4–6] However, some of the factors describing tumour characteristics can only be obtained after surgery.[4–6] As a result, statistical predictive models using conventional preoperative clinical parameters, such as the preoperative Early Recurrence after Surgery for Liver Tumour (ERASL-pre) model, lack sufficient information about tumour characteristics.[7,8] Also, current clinical staging systems, such as Barcelona Clinic Liver Cancer (BCLC), contain inadequate information for predicting recurrence after resection.[7,8] Thus, prognostic indicators toward a deep understanding of preoperative information will help refine and estimate the risk of recurrence and optimise curative strategies.

Aberrant microvasculature of HCC promotes metastatic potential and allows prediction of recurrence.[9] In addition to microvascular invasion (MVI), a well-established prognosticator of recurrence, vessels encapsulating tumour clusters (VETC) has been recently reported as a novel vascular pattern.[10,11] VETC can be released into circulation directly through the anastomosis of VETC itself and peritumour vessels, which is recognised as a distinct mechanism for metastasis and a powerful factor affecting the outcome of HCC.[11–13] Moreover, recent studies reported that the additional use of VETC may help better predict HCC recurrence.[14,15] However, these two distinct vascular patterns can only be assessed in surgical specimens, limiting their clinical utility in the preoperative setting.

Preoperative imaging is an indispensable tool for clinical decision-making in patients with HCC, holding the most immediate promise of providing a reliable non-invasive method for estimating MVI and VETC.[10,16–18] Several peri- or intra-tumoural imaging features deriving from contrast-enhanced images have been highly correlated with MVI.[19,20] In addition, recent studies have described a few imaging features (*e.g.* necrosis) to indicate the VETC pattern.[18,21] However, the prognostic value of imaging-based estimation of these distinct vascular patterns has not been well-defined.[17] Importantly, these easy-to-assess imaging features reflect aggressive biological behaviour, which adds information to the conventional clinical variables, making recurrence prediction more accurate.

Until recently, most preoperative models do not make a further step toward decision-making, such as the initial choice of surgical procedure, a factor which may affect the incidence of recurrence.[22] Theoretically, anatomic resection (AR) is preferred over non-anatomic resection (NAR) for eradicating potential micrometastases, possibly attributed to the aberrant microvasculature.[2,23] However, discrepant results from comparisons between AR and NAR outcomes had led to continued controversy on the optimal type of resection.[24,25] Some recent studies have suggested limited advantages of AR in patients with high micrometastatic burden, such as when aggressive pathological features are presented.[26,27] Ideally, the selection of the optimal type of hepatectomy will benefit from the preoperative knowledge of information on tumour aggressiveness, such as MVI and VETC. However, an approach for recurrence risk stratification incorporating these two distinct vascular patterns has not yet been developed.

Thus, this study aimed at developing a prognostic model that integrates imaging-based surrogates of MVI and VETC as predictors of postoperative recurrence in patients with HCC. Furthermore, whether this model's stratification was associated with postoperative recurrence following AR was assessed.

Patients and methods

This multicentre study was approved by the Institutional Ethics Review Boards of each participating centre. Informed consent was waived given the retrospective nature of the study. The analysis was reported in accordance with the TRIPOD (Transparent reporting of a multivariable prediction model for individual prognosis or diagnosis) guidelines.[28]

Study design and patients

The overall study design is shown in Fig. 1. Data of patients with pathologically identified HCC undergoing curative hepatectomy with tumour-negative resection margins (R0 resection) at five academic medical centres between January 2014 and October 2020 were reviewed. The inclusion criteria were as follows: (1) well-preserved liver function (Child–Pugh grade A or B7 [score ≤7]), (2) available preoperative contrast-enhanced computed tomography (CT) images within 8 weeks before hepatectomy, and (3) a single HCC, or no more than three HCCs, of ≤3 cm. The exclusion criteria were: (1) preoperative anti-cancer treatments,

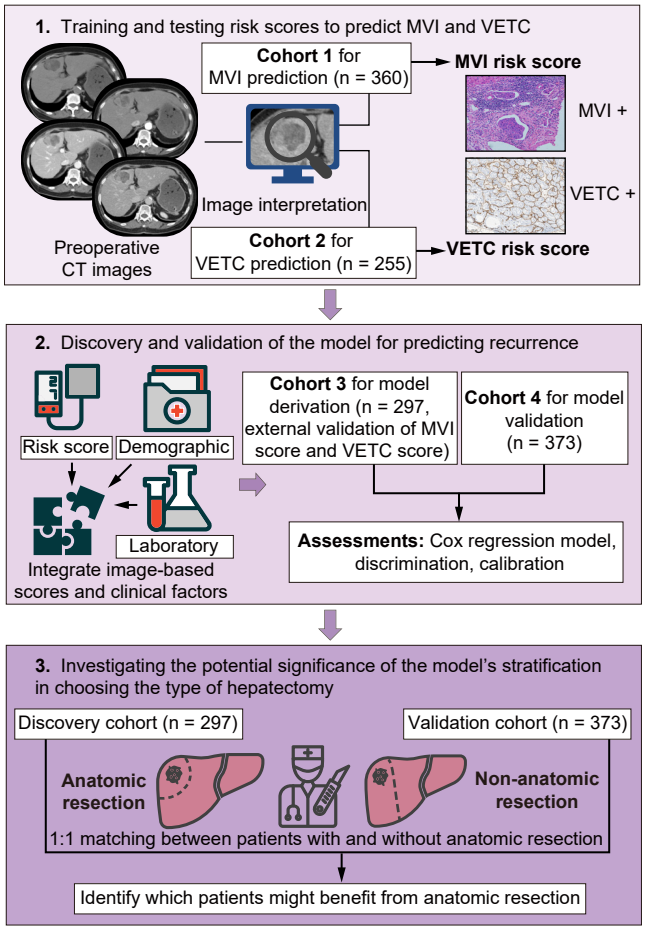

Fig. 1. Study flowchart. FAHZU, the First Affiliated Hospital of Zhejiang University; FAHKMU, the First Affiliated Hospital of Kunming Medical University; JUMC, Jiangnan University Medical Center; MVI, microvascular invasion; VETC, vessels encapsulating tumour clusters; XCHSEU, Xuzhou Central Hospital of Southeast University; ZDHSEU, Zhongda Hospital Southeast University; WPHNMU, the Affiliated Wuxi People's Hospital of Nanjing Medical University; XYHCSU, Xiangya Hospital of Central South University.

(2) the presence of macrovascular invasion or extrahepatic metastasis, and (3) incomplete clinical data.

The detailed patient recruitment process is shown in Fig. S1. The discovery cohort (N = 297) was recruited from three centres, which were Zhongda Hospital Southeast University, Xiangya Hospital of Central South University, and the First Affiliated Hospital of Kunming Medical University. The validation cohort (N = 373) was recruited from the Affiliated Wuxi People's Hospital of Nanjing Medical University and Jiangnan University Medical Center. Demographic information and clinicopathological data from laboratory tests and of liver function were collected from electronic health records. MVI and VETC status of patients in the discovery cohort were additionally evaluated. After resection, all patients were followed up according to the institutional practice, including evaluation of serum alpha-foetoprotein (AFP) levels at 6 months and ultrasound or contrast-enhanced CT every 6–12 months. Recurrence-free survival (RFS) was defined, based on imaging, as the time from surgery to tumour recurrence (including intrahepatic and distant recurrence), death, or censoring at the last follow-up (October 2022).

Using the same criteria, patients from another two centres with available MVI or VETC patterns were enrolled to separately estimate MVI or VETC based on preoperative CT images. These two centres were the First Affiliated Hospital of Zhejiang University (FAHZU) between May 2018 and April 2019 (N = 360) and Xuzhou Central Hospital of Southeast University (XCHSEU) between May 2015 and May 2020 (N = 255).

Evaluation of histopathologic variables

Two liver pathologists independently microscopically viewed all immunostained surgical specimens (Supplementary Methods 1) to determine the histopathological status of VETC and MVI until a consensus was reached. MVI was defined as the presence of tumour cell nests in the portal vein, hepatic vein, and tumour capsular vessel lined by endothelium.[10] VETC referred to sinusoidal blood vessels that encapsulated individual tumour clusters and formed cobweb-like networks on CD34-immunostained sections.[11] The area of VETC was semiquantitatively evaluated from 0% to 100% in 5% units. The optimum cut-off value for VETC predicting RFS was selected by calculating maximally selected rank statistics in the discovery cohort. By doing so, a VETC area ≥5% was defined as VETC-positive.

CT techniques and imaging interpretation

CT acquisition parameters are detailed in Supplementary Methods 2 and Table S1. According to previous imaging analysis for MVI on multiphasic contrast-enhanced CT,[19] the

Table 1. Baseline characteristics.

	n (%)/median (IQR)†				
	Cohorts for the RFS-predicted nomogram				
Variables	Discovery (n = 297)	Validation (n = 373)	*p* value	FAHZU set for MVI (N = 360)	XCHSEU set for VETC (N = 255)
Sex			0.06		
Male	248 (83.5)	289 (77.5)		303 (84.2)	194 (76.1)
Female	49 (16.5)	84 (22.5)		57 (15.8)	61 (23.9)
Age, yrs†	54 (46–62)	57 (47–63)	0.07	59 (51–66)	57 (51–64)
Aetiology			0.13		
None or other	81 (27.3)	123 (33)		95 (26.4)	76 (29.8)
HBV	216 (72.7)	250 (67)		265 (73.6)	179 (70.2)
Child–Pugh class			>0.99		
A	280 (94.3)	352 (94.4)		344 (95.6)	240 (94.1)
B	17 (5.7)	21 (5.6)		16 (4.4)	15 (5.9)
ALBI grade			0.09		
1	195 (65.7)	215 (57.6)		298 (82.8)	195 (76.5)
2/3	102 (34.4)	158 (42.4)		62 (17.2)	60 (23.5)
Cirrhosis			0.38		
Absent	112 (37.7)	128 (34.3)		145 (40.4)	96 (37.6)
Present	185 (62.3)	245 (65.7)		214 (59.6)	159 (62.4)
AFP, ng/ml†			0.93		
≤20	124 (41.8)	156 (41.8)		182 (50.6)	120 (47.1)
20–400	94 (31.6)	122 (32.7)		92 (25.6)	84 (32.9)
>400	79 (26.6)	95 (25.5)		86 (23.9)	51 (20)
ALT, IU/L†	31.9 (21.6–43.7)	28.2 (20.8–45.0)	0.52	27.0 (19.0–39.0)	32.0 (20.0–43.0)
AST, IU/L†	32.2 (21.7–46.6)	30.0 (22.0–44.0)	0.65	27.0 (21.0–36.0)	31 (22.0–38.0)
Albumin, g/L†	40.6 (37.8–43.4)	40.4 (37.3–42.6)	0.08	43.9 (40.3–47.0)	42.5 (39.9–45.5)
Bilirubin, μmol/L†	13.6 (10.5–17.4)	14.3 (11.5–17.8)	0.12	13.1 (10.1–17.7)	14.8 (11.1–18.2)
NLR†	2.18 (1.62–3.12)	2.08 (1.62–2.91)	0.64	2.40 (1.85–3.08)	2.38 (1.73–3.06)
Tumour characteristics					
Tumour size, cm†	4.9 (3.1–7.7)	4.4 (2.9–6.4)	0.13	3.5 (2.3–4.8)	4.8 (3.0–7.0)
Tumour multiplicity	41 (13.8)	37 (9.9)	0.69	30 (8.3)	38 (14.9)
MVI pattern	127 (42.7)	NA		117 (32.5)	NA
VETC pattern	133 (44.8)	NA		NA	112 (43.9)

Differences significant at p <0.05. The ALBI score was computed as −0.085 × (albumin g/L) + 0.66 × $\log_{10}$ (bilirubin μmol/L) and stratified into three grades: grade 1 (≤−2.60), grade 2 (>−2.60 to −1.39), and grade 3 (>−1.39).

AFP, alpha-foetoprotein; ALBI, albumin-bilirubin; ALT, alanine aminotransferase; AST, aspartate aminotransferase; FAHZU, First Affiliated Hospital of Zhejiang University; HBV, Hepatitis B virus; MVI, microvascular invasion; NA, not applicable; NLR, neutrophil–lymphocyte ratio; RFS, recurrence-free survival; VETC, vessels encapsulating tumour clusters; XCHSEU, Xuzhou Central Hospital of Southeast University.

† Continuous variables are presented with median and IQR and compared using the Student's *t* test or Mann-Whitney *U* test; categorical variables are presented with counts and proportions and compared using the Chi-square test or Fisher's exact test.

following four radiological features were evaluated to potentially indicate MVI: (1) arterial peritumoural enhancement, (2) non-smooth tumour margin, (3) capsule disruption, (4) two-trait predictor of venous invasion (TTPVI), and (5) satellite nodules. Since only a few studies investigating imaging findings have indicated VETC as a potential biomarker, the following sets of imaging features were evaluated: (1) different types of dynamic enhancement patterns,[29] categorised as Type-1, homogeneous hypo-enhancement; Type-2, homogeneous hyperenhancement; Type-3, heterogeneous enhancement with septations, and Type-4, heterogeneous enhancement with irregular ring-like structures; (2) proportions of the arterial phase hypovascular component,[30] recorded as <20% or ≥20%; and (3) a set of imaging findings related to aggressive HCC,[17] including the presence of necrosis or severe ischaemia, blood product in mass, corona enhancement, rim arterial phase hyperenhancement, arterial peritumoural enhancement, non-smooth tumour margin, capsule disruption, and intratumoural artery. Tumour size and multiplicity collected from CT reports were analysed for their associations with both MVI and VETC.

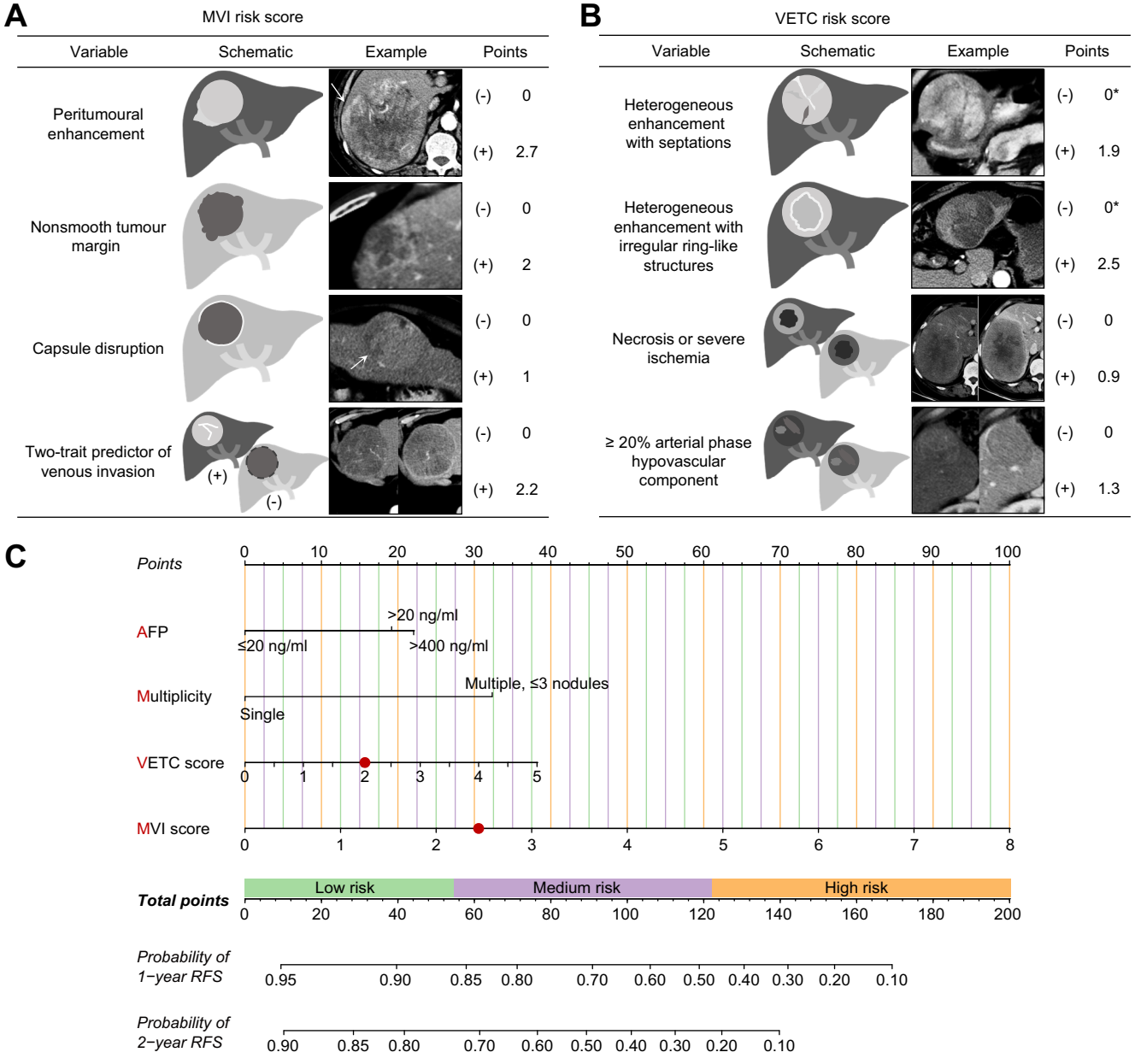

Fig. 2. Derivation of the scores and the constructed nomogram. The derivation of the microvascular invasion (MVI) score (A) and vessels encapsulating tumour clusters (VETC) score (B). 0* denotes homogeneous hypo-enhancement or homogeneous hyperenhancement. The score was calculated as the sum of all points. The nomogram (C) for individual prediction of RFS. The red dots are cut-off points for VETC score (2.05) and MVI score (2.45). AFP, alpha-foetoprotein; MVI, microvascular invasion; RFS, recurrence-free survival VETC, vessels encapsulating tumour clusters.

All contrast-enhanced CT images were uploaded to the imaging management system developed by the Zhongda Hospital Southeast University in anonymised Digital Imaging and Communications in Medicine format. Central imaging review was independently conducted by two radiologists (XM and CX with 6 and 5 years of experience in liver imaging, respectively), who were blinded to all clinical and pathological data. Any discrepancies in radiologic findings were resolved by a third radiologist (YW with 15 years of experience in liver imaging). Interobserver agreement was assessed using Kappa statistics. Details of definitions of imaging features and imaging review training are provided in Supplementary Methods 3.

Construction of CT-based algorithms for MVI and VETC pattern

CT-based algorithms for MVI and VETC patterns were trained and internally validated by splitting data of the FAHZU set (for assessing MVI) and XCHSEU set (for assessing VETC pattern) at a ratio of 3:2. The algorithms were then externally validated in the discovery cohort. The radiological features were investigated for their association with MVI or VETC by logistic regression analysis. Significant variables ($p \leq 0.1$) in the univariable analysis were included in the multivariable analysis. Then, a set of significant radiological features was identified in a backward stepwise selection model with the Akaike information criterion (AIC) being the stopping rule. The MVI and VETC scores were individually formulated using the linear combination of significant factors and their regression coefficients from the multivariable analysis results.[31]

Development of a model for predicting recurrence and benefits of AR

The MVI score, VETC score, and clinical factors were investigated for their association with RFS using univariable Cox regression analyses after performing multiple imputations with five independent draws for missing values. Variables significantly associated with RFS in the univariable analysis ($p \leq 0.1$) were included in the multivariable analysis. A final multivariable Cox model was built through backward stepwise selection with AIC being the stopping rule and displayed as a nomogram. The effect of a variable with the highest coefficient (absolute value) was assigned 100 points, each coefficient in the multivariable regression was assigned a proportional point value. The sum of all point values represented the total point of the nomogram, also named the nomogram-predicted RFS score. The K-adaptive partitioning algorithm with a permutation test was used to find the optimal number of prognostically distinct subgroups and corresponding cut-off point(s) for the nomogram-predicted RFS score.

Furthermore, the ability of the model to predict the benefit of receiving AR was investigated using a post-hoc analysis. Propensity score matching was performed for patients receiving AR *vs.* NAR using 1:1 nearest matching. Detailed analyses of the model's association with benefits of AR are provided in Supplementary Methods 4.

Statistical analysis

Categorical variables were compared using the Chi-square test or Fisher's exact test. Continuous variables were compared using the *t* test or Mann-Whitney *U* test.

Table 2. Univariable and multivariable Cox regression analyses for predicting recurrence-free survival in the discovery cohort.

	Univariable analyses		Multivariable analyses		
Variables	**HR (95% CI)**	***p* value**	**β*(95% CI)**	**HR (95% CI)**	***p* value**
Sex		0.93			
Female	Ref				
Male	1.02 (0.63–1.6)				
Age, yrs	0.99 (0.98–1)	0.17			
Tumour size, cm	1.16 (1.11–1.22)	<0.001			
Tumour multiplicity		<0.001			0.001
No	Ref		Ref	Ref	
Yes	1.94 (1.2–3.0)		0.77 (0.30–1.23)	2.16 (1.36–3.44)	
MVI score	1.39 (1.29–1.50)	<0.001	0.30 (0.22–0.36)	1.35 (1.25–1.46)	<0.001
VETC score	1.23 (1.11–1.37)	<0.001	0.18 (0.07–0.30)	1.20 (1.07–1.34)	0.002
AFP level, ng/ml					
≤20	Ref		Ref	Ref	
20–400	1.73 (1.11–2.69)	<0.001	0.46 (0.01–0.90)	1.58 (1.01–2.46)	0.04
>400	2.72 (1.77–4.18)	<0.001	0.52 (0.08–0.97)	1.69 (1.09–2.63)	0.02
Aetiology		0.24			
None or other					
HBV	1.27 (0.85–1.90)				
Child–Pugh		0.78			
Class A	Ref				
Class B	0.90 (0.42–1.93)				
Cirrhosis		0.07			
Absent	Ref				
Present	1.05 (0.73–1.50)				
ALBI grade		0.90			
1	Ref				
2/3	0.92 (0.64–1.33)				
ALT, IU/L	1.002 (1–1.004)	0.24			
AST, IU/L	1.003 (1–1.005)	0.003			
NLR	1.03 (0.87–1.22)	0.73			

Wald tests were performed to estimate statistical significance of individual variables. Differences significant at $p < 0.05$.
AFP, alpha-foetoprotein; ALBI, albumin-bilirubin; ALT, alanine aminotransferase; AST, aspartate aminotransferase; HBV, hepatitis B virus; HR, hazard ratio; MVI, microvascular invasion; NLR, neutrophil-lymphocyte ratio; VETC, vessels encapsulating tumour clusters.
* β, regression coefficients obtained from multivariable analyses.

The performance of the MVI and VETC scores was measured using the area under receiver operating characteristic curve (AUC) value. Harrell's concordance index (C-index) and time-dependent area under the curve (tdAUC) were used to evaluate the nomogram's discrimination for prognostic prediction. Calibration curves were plotted to compare the predicted recurrence-free probabilities with the actual probabilities. The C-index of the nomogram was compared with that of other prognostic systems or models, including the ERASL-pre model, BCLC stage, Hong Kong Liver Cancer (HKLC) stage, Japan Integrated Staging (JIS) score, China Liver Cancer (CNLC) stage, and the albumin-bilirubin grade-based nomogram (the Ho model).[7,32–36]

All statistics were conducted via R version 4.1.1 (R Foundation for Statistical Computing, Vienna, Austria), details are provided in Supplementary Methods 5. The significance level for the two-tailed testing was defined at 0.05. An online interactive RFS estimate calculator was developed using the R package *shiny*.

Results

Baseline characteristics

A total of 1,285 patients were enrolled in this study. The clinicopathological characteristics of the patients in the discovery cohort, validation cohort, FAHZU set, and XCHSEU set are summarised in Table 1. The demographic and clinicopathological characteristics were similar between the discovery and validation cohorts. The median follow-up time was 28 months (IQR, 26–30 months) for the discovery cohort and 26 months (IQR, 26–28 months) for the validation cohort.

Clinico-radiological characteristics of the patients in the training (N = 209) and internal validation (*JN* = 151) cohorts of the surrogate for MVI are shown in Table S2, and those of patients for the training (N = 153) and internal validation (N = 102) cohorts of the surrogate for VETC are shown in Table S3.

Derivation of MVI and VETC scores

After univariable and multivariable analyses, peritumoural enhancement, non-smooth tumour margin, capsule disruption, and TTPVI were found to be independently associated with the presence of MVI (odds ratio [OR] = 15.60, 7.85, 2.73, and 9.20; regression coefficient = 2.74, 2.04, 1.00, and 2.21, respectively; Table S4). After univariable and multivariable analyses, Type-3 or Type-4 enhancement pattern (Type-1 and -2 as a reference, OR = 6.65 and 12.8, regression coefficient = 1.89 and 2.50, respectively), presence of necrosis (OR = 2.49, regression coefficient = 0.91), and hypovascular enhancement proportion ≥ 20% (OR = 3.63, regression coefficient = 1.29) were found to be independently associated with a higher risk of VETC (Table S5). With the regression coefficient rounded to one decimal, the derived MVI score and VETC score are presented in Fig. 2A and B, respectively.

The interobserver agreement was good to excellent for the radiological features indicated for the MVI and VETC patterns (κ = 0.75–0.85, Table S6). During the training, internal validation, and external validation procedures, the MVI score achieved AUCs of 0.867 (95% CI: 0.813–0.921), 0.851 (95% CI: 0.788–0.913), and 0.883 (95% CI: 0.844–0.923) (Fig. S2A), respectively. The VETC score achieved AUCs of 0.844 (95% CI: 0.781–0.907), 0.834 (95% CI: 0.757–0.912), and 0.842 (95% CI: 0.796–0.888), respectively. The patient distributions according to the MVI and VETC scores are displayed in Tables S7 and S8. For the whole cohort, patients developing extrahepatic recurrence (n = 27) tended to have a higher VETC score (median, IQR: 3.4 [2.2–4.0] vs. 2.2 [1.3–3.8]; $p = 0.02$) and a similar MVI score (median, IQR: 2.2 [0–5.0] vs. 2.0 [0–4.2]; $p = 0.40$) than patients having intrahepatic recurrence (n = 226).

Prognostic model integrating imaging-based scores and clinical factors

Percentages and patterns of missing values are displayed in Fig. S3. All preoperative variables in Table 1 and the MVI and VETC scores were included in the Cox regression analyses. The imaging features used to derive the MVI and VETC scores were similar between the discovery and validation cohorts (Table S9). Serum AFP levels were categorised as ≤20, 20–400, and >400 ng/ml for convenience.[37,38] After univariable and multivariable

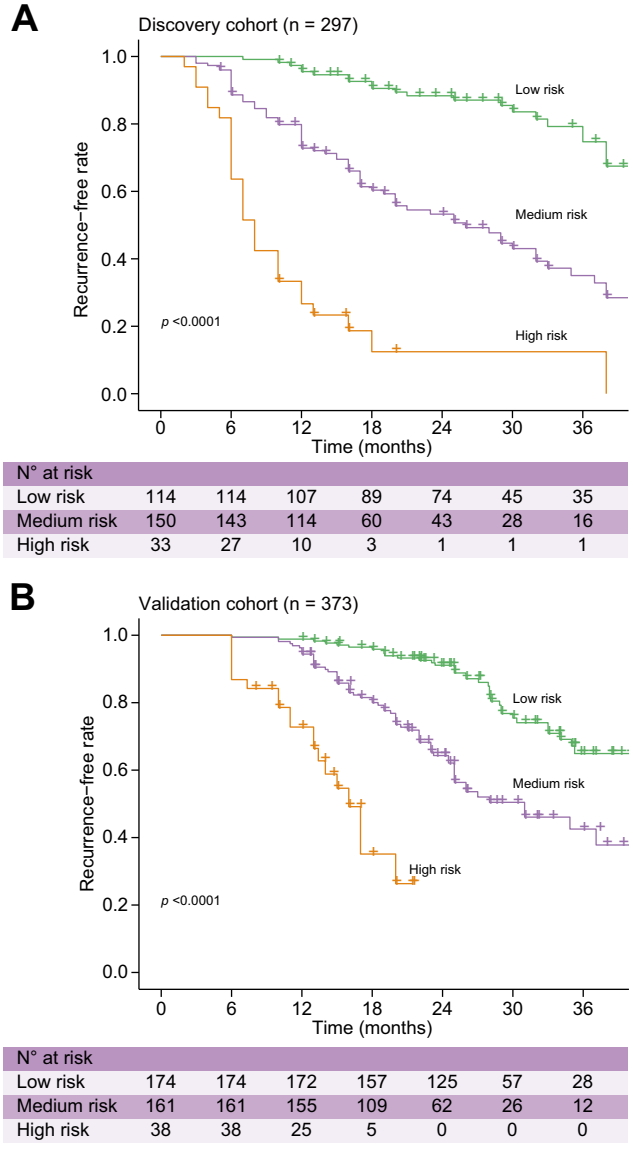

Fig. 3. Kaplan-Meier curves of stratified recurrence-free survival. Discovery cohort (A) and validation cohort (B). Kaplan-Meier curves were compared with the log-rank test. (A–B, high-risk *vs.* medium-risk group p <0.001; medium-risk *vs.* low-risk group p <0.001). Differences significant at p <0.05.

analyses, with results reported as HR with 95% CI: serum AFP level (20–400 *vs.* ≤20 ng/ml, 1.59 [1.02–2.47]; >400 *vs.* ≤20 ng/ml, 1.66 [1.06–2.59]), tumour multiplicity (2.12 [1.34–3.37]), VETC score (1.22 [1.08–1.38]), and MVI score (1.35 [1.25–1.46]) were independently associated with RFS (Table 2). Similarly, the pathological MVI and VETC scores in the multivariable analysis were also proven to be significant prognostic factors (HR = 4.7 and 2.3, respectively, both p <0.001). The model, termed the AMVM (AFP, multiplicity, VETC, and MVI) model, thereafter, achieved C-index of 0.764 (95% CI: 0.721–0.810) and 0.748 (95% CI: 0.707–0.790) in the discovery and validation cohorts, respectively.

An online RFS estimate and risk stratification calculator

Patients were stratified into three prognostically distinct groups, according to the two cut-off points of the nomogram-predicted RFS score (55 and 122) (Fig. 2C) identified by the K-adaptive partitioning algorithm. The online interactive RFS estimate calculator using the variables from the models is available at https://amvmnomogram.shinyapps.io/DynNomapp/. It returns an RFS likelihood at any time between 1 and 60 months after resection and the predicted risk group for individual patients.

In the discovery cohort (Fig. 3A), the median RFS of the three groups from the lowest risk stratum to the highest was 72 (95% CI: 72–99), 26 (95% CI: 20–33), and eight (95% CI: 6–12) months, respectively. Having the low-risk group as a reference, the HR for the medium- and high-risk groups was 3.99 (95% CI: 2.51–6.35; p <0.001) and 16.06 (95% CI: 9.07–28.45; p <0.001), respectively. In the validation cohort (Fig. 3B), the median RFS of the three groups from the lowest risk stratum to the highest was 44 (95% CI: 42.4–66.0), 31 (95% CI: 25.0–45.2), and 16 (13.4–18.0) months. Using the low-risk group as a reference, the HR for the medium- and high-risk groups was 2.96 (95% CI: 1.99–4.39; p <0.001) and 14.66 (95% CI: 7.93–27.09; p <0.001), respectively.

Evaluation of prognostic systems or models

Comparisons of the performance and discrimination between the AMVM model and the prognostic systems or models are shown in Table 3. The tdAUC of the AMVM model was consistently higher than that of the other systems or models over time (Fig. 4A and B). The 1- and 2-year tdAUCs of the AMVM model are shown in Fig. 4C and D, with the calibration curves shown in Fig. S4.

Association between nomogram-predicted stratification and benefit of AR

After matching, the characteristics between patients receiving AR and those receiving NAR were similar within each stratification (Table S10). To explore the predictive value of the nomogram's stratification, the recurrence rates after AR and NAR were compared in the low-, medium-, and high-risk groups. For patients in the nomogram-predicted medium-risk group, AR was associated with an improved RFS (HR = 1.53 [95% CI: 1.08–2.20]; p = 0.017). However, for patients in the nomogram-predicted low- or high-risk group, there was no association between AR and improved RFS (HR = 1.48 [95% CI: 0.85–2.58]; p = 0.17 and HR = 0.98 [95% CI: 0.55–1.77]; p = 0.95) compared with NAR (Fig. 5). Similar results were generated when the above analyses were performed using data without propensity score matching (Fig. S5).

Discussion

The distinct vascular patterns, MVI and VETC, have been recognised as powerful prognostic biomarkers in HCC.[10,14,15] In this large multicentre study, a prognostic model that not only included widely available clinical factors, such as serum AFP and tumour multiplicity, but also pioneeringly introduced the CT-based surrogates of MVI and VETC patterns was proposed. The model displayed improved prognostic performance of RFS than other rival models and routinely used staging systems. Furthermore, the AMVM model stratified patients into three prognostically distinct groups, and AR only reduced the recurrence rate of the medium-risk group.

The current evaluation of the MVI or VETC pattern is based on the histological specimens obtained following surgery, thereby limiting its clinical utility.[10,14] By contrast, assessing these

Table 3. Comparison of the performance and discriminative ability between the AMVM model and other models.

Model	1-yr tdAUC (95% CI)	2-yr tdAUC (95% CI)	C-index (95% CI)
Discovery cohort			
The AMVM model	0.832 (0.750–0.888)	0.835 (0.780–0.890)	0.764 (0.721–0.810)
ERASL-pre model	0.704 (0.633–0.776)	0.734 (0.665–0.803)	0.666 (0.623–0.710)
Ho model	0.647 (0.571–0.722)	0.658 (0.586–0.729)	0.625 (0.575–0.680)
BCLC stage	0.577 (0.535–0.620)	0.561 (0.526–0.596)	0.553 (0.510–0.600)
CNLC stage	0.706 (0.643–0.769)	0.701 (0.637–0.764)	0.650 (0.612–0.690)
HKLC stage	0.641 (0.570–0.712)	0.666 (0.600–0.732)	0.612 (0.558–0.670)
JIS score	0.575 (0.515–0.634)	0.549 (0.496–0.602)	0.549 (0.500–0.600)
Validation cohort			
The AMVM model	0.838 (0.744–0.932)	0.832 (0.781–0.882)	0.748 (0.707–0.790)
ERASL-pre model	0.755 (0.647–0.864)	0.693 (0.623–0.763)	0.685 (0.635–0.740)
Ho model	0.763 (0.617–0.909)	0.646 (0.573–0.720)	0.649 (0.590–0.710)
BCLC stage	0.711 (0.601–0.820)	0.610 (0.566–0.654)	0.598 (0.560–0.640)
CNLC stage	0.719 (0.584–0.853)	0.666 (0.600–0.733)	0.633 (0.579–0.690)
HKLC stage	0.518 (0.401–0.635)	0.578 (0.510–0.647)	0.561 (0.511–0.610)
JIS score	0.700 (0.589–0.811)	0.612 (0.559–0.664)	0.597 (0.555–0.640)

No data were missing in these variables of the comparison models.
BCLC, Barcelona Clinic Liver Cancer; CNLC, China Liver Cancer; ERASL-pre, preoperative Early Recurrence after Surgery for Liver Tumour; HKLC, Hong Kong Liver Cancer; JIS, Japan Integrated Staging tdAUC, time-dependent area under the curve.

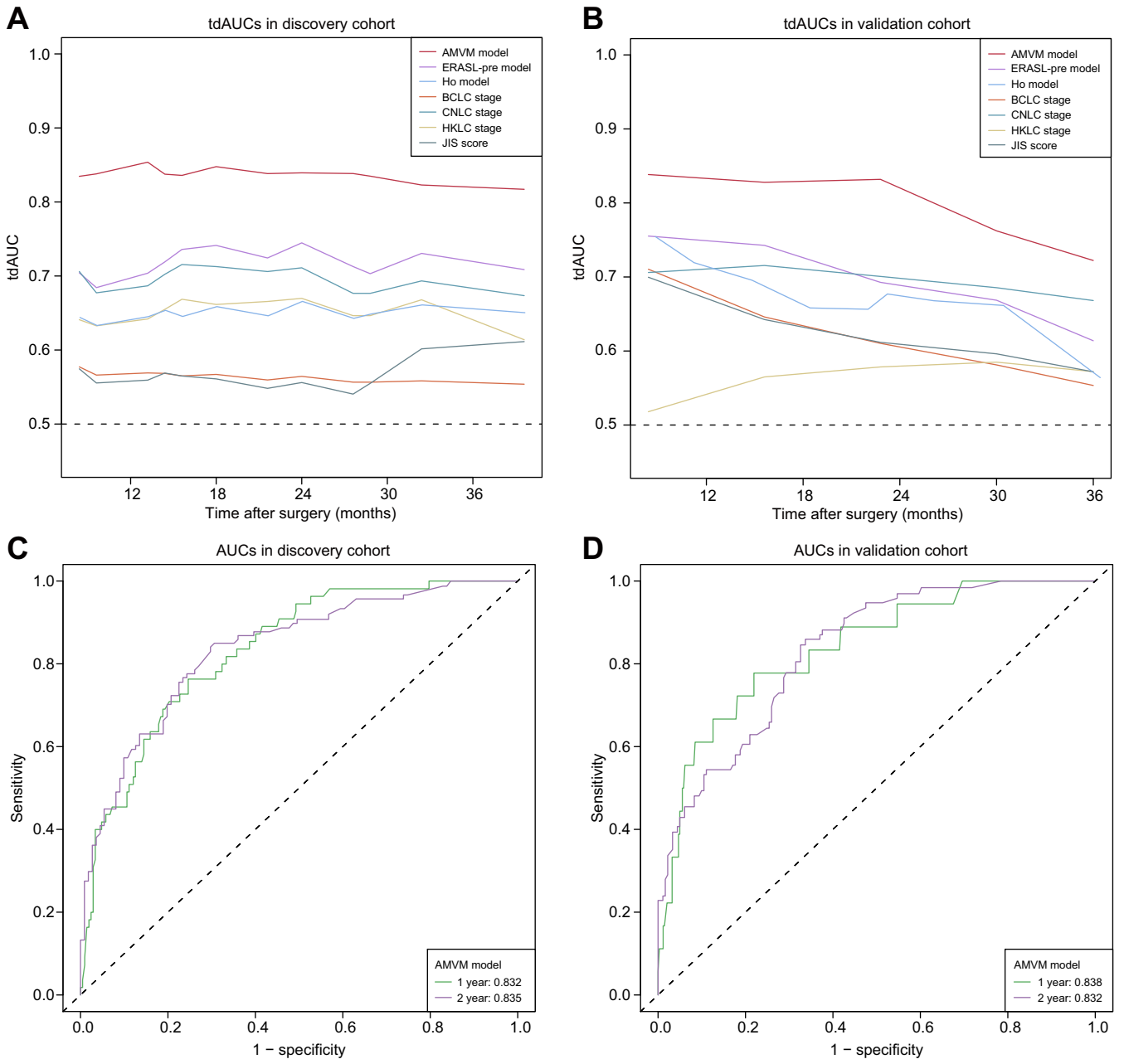

Fig. 4. Time-dependent area under the curve values over time. Time-dependent area under the curve (tdAUC) values over time for the AMVM model and the six prognostic systems or models in the discovery cohort (A) and validation cohort (B). Receiver operating characteristic curves and tdAUC of the AMVM model for predicting 1- and 2-year recurrence in the discovery cohort (C) and validation cohort (D). BCLC, Barcelona Clinic Liver Cancer; CNLC, China Liver Cancer; ERASL-pre, preoperative Early Recurrence after Surgery for Liver Tumour; HKLC, Hong Kong Liver Cancer; JIS, Japan Integrated Staging; tdAUC, time-dependent area under the curve.

distinct vascular patterns using radiological images is a non-invasive approach.[17] Among the proposed imaging features for preoperatively estimating MVI or VETC, the features of arterial peritumoural enhancement, non-smooth tumour margin, capsule disruption, and TTPVI included in the MVI score have been frequently reported;[17,19,20] however, those for the VETC score were not well-defined.[18,21] In the present study where the robustness of the proposed imaging features was verified, the externally validated VETC score indicated that the presence of a Type-3 or Type-4 enhancement pattern, necrosis, and ≥20% arterial phase hypovascular component on CT images were associated with this novel vascular pattern. These features might be associated with the pathomorphological expression of the VETC pattern, which is characterised by compressed peripheral vascular space and subsequent low local blood supply. Although imaging-based estimation is less likely to completely replace the

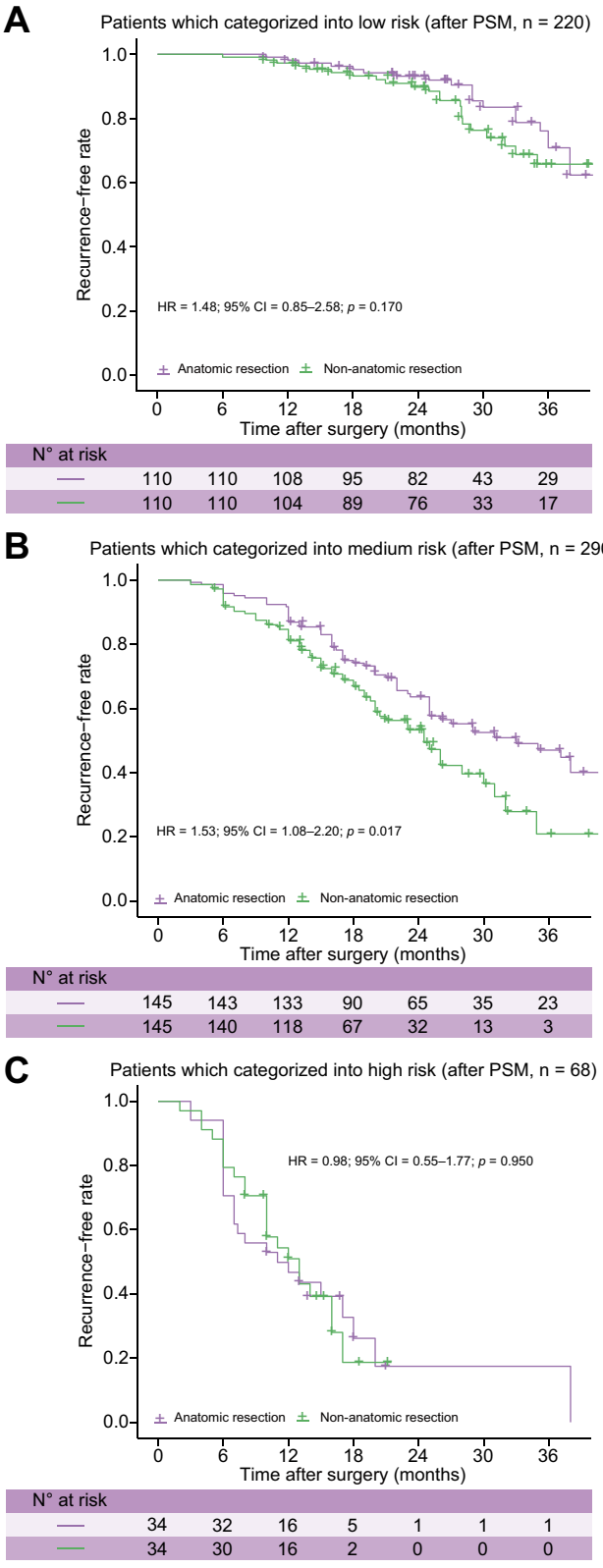

Fig. 5. The relationship between the predicted prognostically distinct groups and the type of hepatectomy in patients with hepatocellular carcinoma after PSM. The recurrence rates between anatomic resection and non-anatomic resection in the nomogram-predicted low-risk group (A), medium-risk group (B), and high-risk group (C) after PSM. The between-group comparisons were made using the Cox model with frail. Differences significant at p <0.05.

current gold standard of pathological evaluation, the MVI and VETC scores demonstrated acceptable performance as potential surrogates. Importantly, these results indicated that both MVI and VETC scores were independently associated with post-resection recurrence, even when adjusting for other clinical variables.

Preoperative models generally fail to incorporate MVI and VETC status, even though these features have been proven as critical determinants of recurrence.[7,8] In the present study, CT-based surrogates of MVI and VETC scores were incorporated into a recurrence prediction model that displayed remarkable performance. It should be noted that, unlike previous studies, tumour size was not included as one of the four significant prognosticators profiling tumour characteristics (i.e. AFP, tumour multiplicity, and imaging-based surrogates of VETC and MVI) of the AMVM model.[6–8] In fact, the factors included in the model may overcome the prognostic limitation of the uni-dimensionality of tumour size, allowing for a more subtle description of tumour biological aggressiveness. Additionally, parameters representing performance status and liver function (*e.g.* albumin-bilirubin grade[39]) were not included; a possible explanation was that most patients enrolled were at very early or early stages and thus had relatively well-preserved performance and liver function. Remarkably, the proposed model informed the risk of MVI and VETC, which may help shed light on the association of tumour aggressiveness and prognosis and may help clinicians define treatment plans, particularly concerning the type of surgical resection.

The study also differed from previous works in that it investigated the potential of the AMVM model to predict the benefits of AR for patients with HCCs. Only the median-risk group showed a significant RFS benefit for patients who received AR *vs.* those who received NAR. However, the results were not significant in the high-risk or low-risk groups. These findings suggest that AR may reduce the risk of tumour recurrence in HCC in patients with moderate micrometastatic burden only. Moreover, given the potential in treating micrometastatic disease of neoadjuvant therapies, this model may provide a rationale for future clinical trial design as it may meet the needs of histologically confirming distinct vascular patterns.

There are some limitations to this study. First, the retrospective nature of the study may have been subject to selection biases despite external validation being conducted to improve reliability. Second, the association between the AMVM model and aggressive subtypes (*e.g.* the macrotrabecular massive subtype) has not been fully understood, and needs to be evaluated by further analyses. Third, this multicentre study was based on HCC data sets of patients within Milan criteria in a hepatitis B virus-predominant area.[3] It will certainly be necessary to verify the transferability of the model.

Conclusions

In summary, information about MVI and VETC included in the AMVM model offers a powerful tool that has been externally validated as a good predictor of post-resection RFS for patients with HCC. Moreover, this model might be useful for selecting candidates who may benefit from AR. These results warrant prospective validation to assess the clinical utility of the model.

Abbreviations

AFP, alpha-foetoprotein; AR, anatomic resection; AUC, area under receiver operating characteristic curve; BCLC, Barcelona Clinic Liver Cancer; CNLC, China liver cancer; tdAUC, time-dependent area under the curve; HCC, hepatocellular carcinoma; HKLC, Hong Kong Liver Cancer; HR, hazard ratio; JIS, Japan Integrated Staging; MVI, microvascular invasion; NAR, non-anatomic resection; OR, odds ratio; RFS, recurrent-free survival; TTPVI, two-trait predictor of venous invasion; VETC, vessels encapsulating tumour clusters.

Financial support

This research was supported by the National Natural Science Foundation of China (NSFC, No. 81830053, 92059202, and 61821002), the Key Research and Development Program of Jiangsu Province (BE2020717), and the National Key R&D Program of China (2021YFF0501504).

Conflicts of interest

The authors declare no conflicts of interest that pertain to this work. Please refer to the accompanying ICMJE disclosure forms for further details.

Authors' contributions

Concept and design: SJ, XM. Data collection: XF, YZ, YS, XL, YL, WX, TX. Experiments and procedures: TT, XM, YW, CX. Statistical analysis: TT, XM, CX. Writing of article: all authors.Critical revision and final approval of the manuscript: all authors.

Data availability statement

The datasets analysed during the current study are available from the corresponding author upon reasonable request.

Supplementary data

Supplementary data to this article can be found online at https://doi.org/10.1016/j.jhepr.2023.100806.

References

Author names in bold designate shared co-first authorship

[1] Sung H, Ferlay J, Siegel RL, Laversanne M, Soerjomataram I, Jemal A, et al. Global Cancer Statistics 2020: GLOBOCAN estimates of incidence and mortality worldwide for 36 cancers in 185 countries. CA Cancer J Clin 2021;71:209–249.
[2] Vogel A, Meyer T, Sapisochin G, Sapisochin G, Salem R, Saborowski A. Hepatocellular carcinoma. Lancet 2022;400:1345–1362.
[3] Zheng R, Zhang S, Zeng H, Wang S, Sun K, Chen R, et al. Cancer incidence and mortality in China, 2016. J Nat Cancer Cent 2022;2:1–9.
[4] Tabrizian P, Jibara G, Shrager B, Schwartz M, Roayaie S. Recurrence of hepatocellular cancer after resection: patterns, treatments, and prognosis. Ann Surg 2015;261:947–955.
[5] Nahon P, Vibert E, Nault JC, Ganne-Carrié N, Ziol M, Seror O. Optimizing curative management of hepatocellular carcinoma. Liver Int 2020;40(Suppl 1):109–115.
[6] Ivanics T, Murillo Perez CF, Claasen MPAW, Patel MS, Morgenshtern G, Erdman L, et al. Dynamic risk profiling of HCC recurrence after curative intent liver resection. Hepatology 2022;76:1291–1301.
[7] Chan AWH, Zhong J, Berhane S, Toyoda H, Cucchetti A, Shi K, et al. Development of pre and post-operative models to predict early recurrence of hepatocellular carcinoma after surgical resection. J Hepatol 2018;69:1284–1293.
[8] Shim JH, Jun MJ, Han S, Li R. Prognostic nomograms for prediction of recurrence and survival after curative liver resection for hepatocellular carcinoma. Ann Surg 2015;261:939–946.
[9] **Zhang Q**, **Wu J**, Bai X, Liang T. Evaluation of intra-tumoral vascularization in hepatocellular carcinomas. Front Med (Lausanne) 2020;7:584250.
[10] Erstad DJ, Tanabe KK. Prognostic and therapeutic implications of microvascular invasion in hepatocellular carcinoma. Ann Surg Oncol 2019;26:1474–1493.
[11] **Fang JH**, **Zhou HC**, Zhang C, Shang LR, Zhang L, Xu J, et al. A novel vascular pattern promotes metastasis of hepatocellular carcinoma in an epithelial-mesenchymal transition-independent manner. Hepatology 2015;62:452–465.
[12] Zhou HC, Liu CX, Pan WD, Shang LR, Zheng JL, Huang BY, et al. Dual and opposing roles of the androgen receptor in VETC-dependent and invasion-dependent metastasis of hepatocellular carcinoma. J Hepatol 2021;75:900–911.
[13] **Renne SL**, **Woo HY**, **Allegra S**, Rudini N, Yano H, Donadon M, et al. Vessels encapsulating tumor clusters (VETC) is a powerful predictor of aggressive hepatocellular carcinoma. Hepatology 2020;71:183–195.
[14] Lu L, Wei W, Huang C, Li S, Zhong C, Wang J, et al. A new horizon in risk stratification of hepatocellular carcinoma by integrating vessels that encapsulate tumor clusters and microvascular invasion. Hepatol Int 2021;15:651–662.
[15] Lin WP, Xing KL, Fu JC, Ling YH, Li SH, Yu WS, et al. Development and validation of a model including distinct vascular patterns to estimate survival in hepatocellular carcinoma. JAMA Netw Open 2021;4:e2125055.
[16] Bruix J, Reig M, Rimola J, Forner A, Burrel M, Vilana R, et al. Clinical decision making and research in hepatocellular carcinoma: pivotal role of imaging techniques. Hepatology 2011;54:2238–2244.
[17] Fowler KJ, Burgoyne A, Fraum TJ, Hosseini M, Ichikawa S, Kim S, et al. Pathologic, molecular, and prognostic radiologic features of hepatocellular carcinoma. Radiographics 2021;41:1611–1631.
[18] Feng Z, Li H, Zhao H, Jiang Y, Liu Q, Chen Q, et al. Preoperative CT for characterization of aggressive macrotrabecular-massive subtype and vessels that encapsulate tumor clusters pattern in hepatocellular carcinoma. Radiology 2021;300:219–229.
[19] Renzulli M, Brocchi S, Cucchetti A, Mazzotti F, Mosconi C, Sportoletti C, et al. Can current preoperative imaging be used to detect microvascular invasion of hepatocellular carcinoma? Radiology 2016;279:432–442.
[20] Lee S, Kim SH, Lee JE, Sinn DH, Park CK. Preoperative gadoxetic acid-enhanced MRI for predicting microvascular invasion in patients with single hepatocellular carcinoma. J Hepatol 2017;67:526–534.
[21] **Chen FM**, **Du M**, Qi X, Bian L, Wu D, Zhang SL, et al. Nomogram estimating vessels encapsulating tumor clusters in hepatocellular carcinoma from preoperative gadoxetate disodium-enhanced MRI. J Magn Reson Imaging 2023;57:1893–1905.
[22] Shindoh J, Kobayashi Y, Umino R, Kojima K, Okubo S, Hashimoto M, et al. Successful anatomic resection of tumor-bearing portal territory delays long-term stage progression of hepatocellular carcinoma. Ann Surg Oncol 2021;28:844–853.
[23] Shindoh J, Makuuchi M, Matsuyama Y, Mise Y, Arita J, Sakamoto Y, et al. Complete removal of the tumor-bearing portal territory decreases local tumor recurrence and improves disease-specific survival of patients with hepatocellular carcinoma. J Hepatol 2016;64:594–600.
[24] Moris D, Tsilimigras DI, Kostakis ID, Ntanasis-Stathopoulos I, Shah KN, Felekouras E, et al. Anatomic versus non-anatomic resection for hepatocellular carcinoma: a systematic review and meta-analysis. Eur J Surg Oncol 2018;44:927–938.
[25] Su CM, Chou CC, Yang TH, Lin YJ. Comparison of anatomic and non-anatomic resections for very early-stage hepatocellular carcinoma: the importance of surgical resection margin width in non-anatomic resection. Surg Oncol 2021;36:15–22.
[26] Jung DH, Hwang S, Lee YJ, Kim KH, Song GW, Ahn CS, et al. Small hepatocellular carcinoma with low tumor marker expression benefits more from anatomical resection than tumors with aggressive biology. Ann Surg 2019;269:511–519.
[27] Okamura Y, Sugiura T, Ito T, Yamamoto Y, Ashida R, Ohgi K, et al. Anatomical resection is useful for the treatment of primary solitary hepatocellular carcinoma with predicted microscopic vessel invasion and/or intrahepatic metastasis. Surg Today 2021;51:1429–1439.
[28] Collins GS, Reitsma JB, Altman DG, Moons KG. Transparent reporting of a multivariable prediction model for individual prognosis or diagnosis (TRIPOD): the TRIPOD statement. BMJ 2015;350:g7594.
[29] Kawamura Y, Ikeda K, Hirakawa M, Yatsuji H, Sezaki H, Hosaka T, et al. New classification of dynamic computed tomography images predictive of malignant characteristics of hepatocellular carcinoma. Hepatol Res 2010;40:1006–1014.

[30] Rhee H, Cho ES, Nahm JH, Jang M, Chung YE, Baek SE, et al. Gadoxetic acid-enhanced MRI of macrotrabecular-massive hepatocellular carcinoma and its prognostic implications. J Hepatol 2021;74:109–121.
[31] Sullivan LM, Massaro JM, D'Agostino Sr RB. Presentation of multivariate data for clinical use: the Framingham Study risk score functions. Stat Med 2004;23:1631–1660.
[32] Reig M, Forner A, Rimola J, Ferrer-Fàbrega J, Burrel M, Garcia-Criado Á, et al. BCLC strategy for prognosis prediction and treatment recommendation: the 2022 update. J Hepatol 2022;76:681–693.
[33] **Yau T**, **Tang VY**, **Yao TJ**, Fan ST, Lo CM, Poon RT. Development of Hong Kong Liver Cancer staging system with treatment stratification for patients with hepatocellular carcinoma. Gastroenterology 2014;146:1691–1700.e1693.
[34] Kudo M, Chung H, Osaki Y. Prognostic staging system for hepatocellular carcinoma (CLIP score): its value and limitations, and a proposal for a new staging system, the Japan Integrated Staging Score (JIS score). J Gastroenterol 2003;38:207–215.
[35] **Zhou J**, **Sun H**, **Wang Z**, Cong W, Wang J, Zeng M, et al. Guidelines for the diagnosis and treatment of hepatocellular carcinoma (2019 Edition). Liver Cancer 2020;9:682–720.
[36] **Ho SY**, **Hsu CY**, Liu PH, Hsia CY, Su CW, Huang YH, et al. Albumin-bilirubin (ALBI) grade-based nomogram to predict tumor recurrence in patients with hepatocellular carcinoma. Eur J Surg Oncol 2019;45:776–781.
[37] Ma WJ, Wang HY, Teng LS. Correlation analysis of preoperative serum alpha-fetoprotein (AFP) level and prognosis of hepatocellular carcinoma (HCC) after hepatectomy. World J Surg Oncol 2013;11:212.
[38] Yang SL, Liu LP, Yang S, Liu L, Ren JW, Fang X, et al. Preoperative serum α-fetoprotein and prognosis after hepatectomy for hepatocellular carcinoma. Br J Surg 2016;103:716–724.
[39] Johnson PJ, Berhane S, Kagebayashi C, Satomura S, Teng M, Reeves HL, et al. Assessment of liver function in patients with hepatocellular carcinoma: a new evidence-based approach-the ALBI grade. J Clin Oncol 2015;33:550–558.